BIOCELL
2022 46(12): 2659-2669

Tech Science Press

ZBTB7A governs 2-DG-inhibited glycolysis by regulating GLUT1 in nasopharyngeal carcinoma

Fei LIU[1]; Jiazhang WEI[2]; Jiao LAN[1]; Yongli WANG[2]; Jianxiang YE[3]; Cheng SU[1]; Mingzheng MO[1]; Fengzhu TANG[2]; Bing LI[2]; Min LI[2]; Weiming DENG[2]; Linsong YE[2]; Wenlin HUANG[2]; Jingjin WENG[2]; Wei JIAO[1,*]; Shenhong QU[2,*]

[1] Research Center of Medical Sciences, The People's Hospital of Guangxi Zhuang Autonomous Region, Guangxi Academy of Medical Sciences, Nanning, 530021, China
[2] Department of Otolaryngology & Head and Neck, The People's Hospital of Guangxi Autonomous Region, Guangxi Academy of Medical Sciences, Nanning, 530021, China
[3] Department of Medical Oncology, Guangxi Medical University Cancer Hospital, Nanning, 530021, China

Key words: Nasopharyngeal carcinoma, ZBTB7A, GLUT1, Glycolysis, 2-DG

Abstract: Our previous studies suggested a potential interaction between the POK erythroid myeloid ontogenic factor ZBTB7A and glucose transporter 1 (GLUT1) in nasopharyngeal carcinoma (NPC). This study was designed to confirm the interaction and further evaluate the precise mechanism by which ZBTB7A and GLUT1 regulate NPC development. The binding sites between ZBTB7A and the promoter of GLUT1 were predicted by bioinformatics. Gene expression was measured by quantitative real-time polymerase chain reaction (qPCR), western blotting, and immunohistochemistry. The activities of key glycolysis enzymes, including hexokinase (HK), pyruvate kinase (PK), lactate dehydrogenase (LDH), and lactate, were detected using specific enzyme-linked immunosorbent assay kits. The connection between ZBTB7A and GLUT1 was analyzed by dual-luciferase reporter assay and chromatin immunoprecipitation–qPCR. The vitality, proliferation, and tumorigenicity of the cells expressing different levels of ZBTB7A were tested by adding the glycolysis inhibitor 2-deoxy-D-glucose (2-DG), followed by MTT, colorimetric focus forming, and xenograft assays, respectively. Our results showed that high expression of GLUT1 was associated with late-stage NPC. After constructing stably transfected cells with lentiviruses, ZBTB7A was effectively knocked down in 5-8F cells (RNAi-5-8F) and overexpressed in 6-10B cells (ZBTB7A-6-10B). The up- or downregulation of GLUT1 secondary to ZBTB7A changes was also limited. The vitality and proliferation of the cells expressing low ZBTB7A were notably blocked by 2-DG. The cells expressing high ZBTB7A were not very sensitive to 2-DG. The growth of RNAi-5-8F xenografts was strongly suppressed by 2-DG. The activities of HK, PK, and LDH were suppressed by 2-DG in the cells expressing low ZBTB7A. RNAi-5-8F cells had the lowest 2-DG-induced lactate production. ZBTB7A directly suppressed the promoter region of GLUT1 to regulate GLUT1 expression. Thus, ZBTB7A controls the 2-DG-induced inhibition of glycolysis by affecting GLUT1.

Introduction

Nasopharyngeal carcinoma (NPC) is prevalent in southern China, especially in Guangdong and Guangxi Provinces (Xu *et al.*, 2019; Chen *et al.*, 2021a). The estimated number of new cases in China was almost half of the total cases worldwide in 2018 (Xu *et al.*, 2019). Although chemotherapy is an important method among NPC therapies (Chen *et al.*, 2021b; Liu *et al.*, 2021c), some drugs cannot play an effective role because of the complex regulation of pivotal genes (Peng *et al.*, 2019; Zhang *et al.*, 2019). Therefore, precise chemotherapy should be devised by exploring resistance mechanisms (Liu *et al.*, 2021b; Zhu *et al.*, 2020; Hong *et al.*, 2020).

Zinc finger and BTB domain-containing protein 7A ZBTB7A, also named POK erythroid myeloid ontogenic factor (Pokemon), shows opposing functions in different cancers. As a tumor suppressor, ZBTB7A inhibits the progression of endometrial cancer, oral squamous cell carcinoma, gastric cancer, melanoma, and prostate cancer (Geng *et al.*, 2020; Yeh *et al.*, 2020; Sun *et al.*, 2018; Liu *et al.*, 2015; Wang *et al.*, 2013). As an oncogene, ZBTB7A promotes the deterioration of colorectal cancer, breast cancer, osteosarcoma, and non-small-

*Address correspondence to: Shenhong Qu, qshdoctor@163.com; Wei Jiao, gxjw2005@gmail.com
Received: 30 March 2022; Accepted: 24 June 2022

Doi: 10.32604/biocell.2022.022886

cell lung cancer (Wang *et al*., 2020; Mao *et al*., 2019; Zhang *et al*., 2019; Zhao *et al*., 2017; Kong *et al*., 2016).

Although the expression levels of ZBTB7A in NPC tissues and cell lines were higher than in their respective controls (Jiao *et al*., 2013; Liu *et al*., 2019), ZBTB7A has shown complex roles in NPC. Stable overexpression and transient knockdown of ZBTB7A promoted and suppressed the progression of NPC cells, respectively (Liu *et al*., 2019; Liu *et al*., 2017; Liu *et al*., 2018). Notably, stable knockdown of ZBTB7A also promoted NPC development (Liu *et al*., 2018). Expression profiles of long noncoding RNA and messenger RNAs have indicated that some suppressed oncogenes can vicariously maintain the development of NPC cells with a decrease in ZBTB7A (Liu *et al*., 2019). The differentially expressed mRNAs are mainly involved in carbohydrate and lipid metabolism. We have found that key genes of lipid pathways, such as sterol regulatory element-binding transcription factor 1 (SREBF1) and fatty acid synthase (Liu *et al*., 2019; Liu *et al*., 2021a), are involved, but a role for glucose transporter 1 (GLUT1) in NPC was not validated in our study (Liu *et al*., 2019).

GLUT1 is also called solute carrier family member 1 (SLC2A1). GLUT1 expression was higher in head and neck squamous cell carcinoma (HNSCC) than in normal tissues (Fig. S1). Its expression in the T1 stage of HNSCC was lower than in the T4 stage (Fig. S2). Survival analyses did not show a difference (Figs. S3–S5). The correlation between ZBTB7A and GLUT1 was seen in HNSCC (Fig. S6). No statistical differences were found between gene set enrichment (GSE)12452 and GSE64634, which included NPC and normal tissues (Figs. S7A and S7B). Although a significant difference was observed in GSE13597, three normal tissues were not sufficient to support any firm conclusion (Fig. S7C).

Although NPC is a kind of HNSCC, it shows evident differences from other HNSCCs. For example, most tissues of NPC have unique characteristics of undifferentiated nonkeratinizing in endemic regions (Badoual, 2022). According to the National Comprehensive Cancer Network guidelines, NPC definitely differs from HNSCC. Therefore, there are probably gene expression differences between NPC and HNSCC. Bioinformatic analysis of GLUT1 in HNSCC also did not directly reveal the role of GLUT1 in NPC.

To further explore the role of GLUT1 in NPC and the relationship between ZBTB7A and GLUT1, we continued to explore the target gene as a continuous collection of NPC and control tissues.

Materials and Methods

Bioinformatic analysis

In HNSCC, the assessments of GLUT1 expression, clinical correlates, and the association between ZBTB7A and GLUT1 were performed using Gene Expression Profiling Interactive Analysis (http://gepia.cancer-pku.cn/) and The Cancer Genome Atlas (TCGA) databases (https://www.cancer.gov/about-nci/organization/ccg/research/structural-genomics/tcga). GLUT1 expression was detected by RNA sequencing (RNA-seq) on 502 HNSCC and 44 normal tissues (Figs. S1–S6). In NPC, GLUT1 expression from GSE12452, GSE13597, and GSE64634 was assessed using the Gene Expression Omnibus (GEO) database (https://www.ncbi.nlm.nih.gov/geo/). In total, 68 (respectively, 31, 25, 12) NPC and 17 (10, 3, 4) normal nasopharyngeal tissues were detected by mRNA expression profiling arrays (Fig. S7). Potential connections between ZBTB7A and the promoter region of GLUT1 were predicted by JASPAR (https://jaspar.genereg.net/).

Clinical samples

Eighty NPC and 40 chronic rhinitis tissues were collected from July 2016 to July 2019 for quantitative PCR. GLUT1 is expressed in some tissues (Liu *et al*., 2019). Twenty-four tissues samples were collected from patients with NPC for immunohistochemistry (IHC). Ten tissue samples were acquired from patients with early-stage (I + II) NPC. Fourteen tissue samples were acquired from patients with late-stage (III + IV) NPC. The tumors were staged according to the Union for International Cancer Control (2010, 7th edition) for NPC. The clinical samples were approved by the Ethics Committee of The People's Hospital of Guangxi Zhuang Autonomous Region, Guangxi Academy of Medical Sciences (Ethical Application Ref: Keyan-Guangxi-Keji-2016-20). We received written consent from all participants in our study. They volunteered to participate in the study, and their information was not published here.

Cell culture and transfection

Considering the high efficiency and low toxicity of lentivirus in cell transfection assays (Sena-Esteves and Gao, 2018; Stepanenko and Heng, 2017), we reconstructed lentivirus vectors of ZBTB7A and retained the effective sequences for RNA interference (RNAi) and overexpression from old plasmids (Liu *et al*., 2019; Liu *et al*., 2018). Following the instructions from Genechem (Shanghai, China), the lentiviruses were stably transfected into 5-8F and 6-10B cells. The cells stably transfected with empty lentiviruses were used as negative controls (NCs). The sublines were named RNAi-5-8F, NC-5-8F, ZBTB7A-6-10B, and NC-6-10B and cultured in Roswell Park Memorial Institute 1640 medium supplemented with 10% fetal bovine serum (Gibco, Thermo Fisher Scientific, Waltham, USA). The immortalized nasopharyngeal epithelial cell line NP69 was cultured in a keratinocyte serum-free medium with 5% bovine pituitary extract and recombinant epidermal growth factor (Gibco).

Quantitative real-time polymerase chain reaction (qPCR)

Total RNA of the tissues and cells was extracted using TRIzol reagent (Invitrogen, Carlsbad, USA). Reverse transcription and qPCR were performed on 80 tissues (60 NPC tissues and 20 controls) (Liu *et al*., 2019). The RNAs extracted from cell lines and 40 additional tissues (20 NPC tissues and 20 controls) were reverse transcribed by a SuperScript TM III Reverse Transcriptase Kit (Invitrogen). The primer sequences of GLUT1 and glyceraldehyde-3-phosphate dehydrogenase (GAPDH) have been described previously (Liu *et al*., 2019). GAPDH was used as the internal control. The reaction program and analysis of the results were also performed as described previously (Liu *et al*., 2019).

Western blotting (WB)

The cell lines were lysed with radioimmunoprecipitation buffer (Beyotime, Shanghai, China) and the protease inhibitor phenylmethanesulfonyl fluoride (Beyotime). Total protein (20 μg) was separated by sodium dodecyl sulfate-polyacrylamide gel electrophoresis and transferred onto 0.22 μm nitrocellulose membranes (Millipore, Billerica, USA). Membranes were incubated with primary antibodies (1:500 dilution; catalog no. ab70208, anti-ZBTB7A antibody from Abcam [Cambridge, UK]; 1:500 dilution, catalog no. SAB2700223, anti-GLUT1 antibody from Sigma-Aldrich [Saint Louis, USA]; 1:1000 dilution, catalog no. AA128, anti-human beta-actin [ACTB] antibody from Beyotime). Then they were incubated with anti-rabbit or anti-mouse antibodies as described previously (Liu *et al.*, 2021a). ACTB was used as a loading control.

3-(4,5-Dimethyl-2-thiazolyl)-2,5-diphenyl-2-H-tetrazolium bromide (MTT) assay

5-8F and 6-10B stably transfected cells were seeded in 96-well plates at a density of 1500 cells/well and cultured with 300 μg/mL 2-deoxy-D-glucose (2-DG) or phosphate-buffered saline (PBS) for 24, 48, 72 or 96 h. The cells were then incubated with 0.5% MTT (Sigma-Aldrich) and lysed with dimethyl sulfoxide (Sigma-Aldrich). The absorbance was detected by a Synergy H1 microplate reader (BioTek Instruments, Winooski, USA).

Colorimetric focus forming assay

Stably transfected 5-8F and 6-10B cells were seeded in 6-well plates at 100 cells/well and cultured with 300 μg/mL 2-DG and PBS for 2 weeks. The cells were fixed with 100% methanol and dyed with 5% crystal violate (Dama Chemical Reagent Factory, Tianjing, China).

Measurements of hexokinase (HK), pyruvate kinase (PK), lactate dehydrogenase (LDH), and lactate production

Stably transfected 5-8F and 6-10B cells were seeded in 6-well plates (2×10^5 cells). During incubation at 37°C for 3 days, we added 300 μg/mL of the inhibitor of glycolysis, 2-DG (Solarbio, Beijing, China), to the medium (negative control: PBS). Then the cells were digested with 0.25% trypsin, washed with PBS, and sonicated by ultrasound (Vibra-Cell™ processor, Sonics, Newtown, USA) on ice. According to the manufacturer's instructions (Solarbio, Beijing, China), the extracts were processed and measured by a Synergy H1 microplate reader. To assess HK, PK, LDH, and lactate production, the absorbances were measured at 340 nm, 340 nm, 450 nm, and 570 nm, respectively. The activities of HK, PK, and LDH and the concentration of lactate were calculated as instructed by the kits. The activities of HK, PK, and LDH in the control group were normalized to 1.0.

Dual-luciferase reporter assay

GLUT1 wild-type (WT) or mutant (Mut) was cotransfected with the ZBTB7A overexpression plasmid or NC plasmid into NPC cells. Following the instructions of the Dual-Luciferase® Reporter Assay System (Promega, Madison, USA), relative luciferase activity was screened by a Synergy H1 microplate reader.

Chromatin immunoprecipitation- quantitative real-time polymerase chain reaction (ChIP–qPCR)

ChIP was performed based on a previously described method (DeCaprio and Kohl, 2020). A total of 7×10^6 NPC cells were subjected to two-step dual crosslinking. Immunoprecipitated protein–DNA complexes were obtained with anti-ZBTB7A antibody (1:200 dilution; Abcam, ab175918). Purified DNA was analyzed by qPCR with CFX Connect (Bio-Rad, Hercules, USA) and SYBR Green Mix (Vazyme, Nanjing, China). The following primer pairs (forward and reverse) were used: GLUT1, 5'-TGTAAGGCAAGCTGGGATG-3' and 5'-GGTCTTTCTACAACCCTACGAG-3'; ACTB, 5'-TCCTTCCTGGGCATGGAGT-3' and 5'-CAGGAGGAG-CAATGATCTTGAT-3'.

Xenografts

A total of 5×10^6 RNAi-5-8F and NC-5-8F cells were subcutaneously injected into the left and right flanks of BALB/c nude mice (female, 4 weeks old; average weight, 16.104 ± 0.798 g; Guangxi Medical University Laboratory Animal Centre) because of their stronger vitality and proliferation abilities than those of the 6-10B sublines. Based on the table of random numbers, our team members randomly divided 24 mice into four groups (6 mice/group/cage) and injected 2 g/kg 2-DG (dissolved in PBS) or PBS into the abdomen of mice every other day starting 3 days after the injection of the cells. The sample size of 24 mice was determined by calculating statistical differences and the maximum number of mice in a cage. RNAi-5-8F- and NC-5-8F-injected PBS were used as the control groups. We gently touched the mouse's back to alleviate their tenseness before injection of cells, 2-DG, or PBS. When they were 8 weeks old, the anesthetized mice were sacrificed through cervical dislocation. To alleviate pain, the mice were anesthetized with 10% chloral hydrate at a concentration of 4 mL/100 g before sacrifice. The volumes and weights of tumor tissues were measured. Tumor volume was calculated using the formula $V = (\pi/6)\ (d1 \times d2)^{3/2}$. The volumes were not too large to influence the survival of mice. All animal procedures were conducted based on the Guidelines for the Care and Use of Laboratory Animals and were approved by the Ethics Committee of Guangxi Medical University Laboratory Animal Centre (202007059). The BALB/c mice used in this study were specific pathogen-free (SPF) animals. They were raised in independent ventilation cages (IVC, Tecniplast, Via I Maggio, 6-21020 BUGUGGIATE (VA), Italia). The temperature was 20–25°C, and the atmosphere was 20–50 Pa. The light/dark cycle was 10/14 h. The food was sterilized by autoclaving. The water was purified and sterilized. BALB/c nude mice were used because they are an ideal animal model simulating neoplasia because of their immune deficiency.

IHC

The clinical NPC and mouse xenograft tissues were dissected and fixed in 4% paraformaldehyde overnight. A 3 μm section was deparaffinized in xylene and rehydrated through descending graded concentrations of ethanol. After antigen retrieval, nonspecific binding sites were blocked with bovine serum albumin (BSA, Servicebio) for 30 min at room

temperature. The sections were incubated with GLUT1 primary antibody (1:300 dilution, catalog No. GB11215; Servicebio, Wuhan, China) overnight at 4°C. After being washed with PBS (pH 7.4), they were incubated with a secondary antibody (1:200 dilution, catalog No. GB23303; Servicebio) for 50 min at room temperature. DAB was added to the circle after the sections were washed and slightly dried. The nucleus stained with hematoxylin was blue, and those with DAB showed up brownish-yellow. The sections were observed under a BX51 fluorescence microscope (Olympus, Tokyo, Japan). The average staining intensity (average optical density, AOD), reflecting the average level of positive signal, was analyzed by ImageJ (National Institutes of Health, Bethesda, USA) (Zhang *et al.*, 2021).

Statistical analysis

Experimental data were analyzed by SPSS 13.0 (IBM, Armonk, USA), Prism 5 (GraphPad, San Diego, USA), and SigmaPlot 12.5 (Systat Software, San Jose, USA). Statistical differences between the two groups were estimated by the two-tailed Student's *t*-test. To analyze the scatter plot of tissue qPCR data, the Mann–Whitney U test was used if the variances were significantly different by the *F* test. $P < 0.05$ was considered to be statistically significant.

Results

High expression of GLUT1 is associated with NPC tissues, especially late-stage NPC

Although a difference was not seen between 60 NPC and 20 control tissues (Liu *et al.*, 2019), we continued to collect samples and detected the expression of GLUT1 via qPCR. Analysis by qPCR revealed that GLUT1 expression in 80 NPC tissues was higher than in 40 control (Fig. 1A). GLUT1 expressions of 14 late-stage NPC tissues were higher than those of 10 early-stage tissues, as shown by IHC (Figs. 1B and 1C).

ZBTB7A and GLUT1 expression are negatively associated in NPC cells

ZBTB7A was effectively knocked down or overexpressed in cells stably transfected with lentiviruses, as intended. WB results reveal that the stable knockdown and overexpression of ZBTB7A upregulated and downregulated the expression of GLUT1, respectively, as shown by WB (Figs. 2A–2C).

The vitality and proliferation of NPC cells expressing low ZBTB7A are markedly blocked by 2-deoxy-d-glucose in vitro

The vitality and proliferation of RNAi-5-8F and ZBTB7A-6-10B cells were, respectively, stronger than those of NC-5-8F and NC-6-10B cells. These results were similar to those reported in prior studies (Liu *et al.*, 2019; Liu *et al.*, 2018). The vitality and proliferation capabilities of the cells were weakened by 2-DG; interestingly, these capabilities of RNAi-5-8F with 2-DG were weaker than those of other cells with 2-DG or PBS (Figs. 3A–3D).

The activities of key glycolysis enzymes are notably blocked by 2-DG

To clarify whether glycolysis in the cells was inhibited by 2-DG, we measured the relative activities of HK, PK, LDH, and lactate production in the cells treated with 2-DG or PBS. Compared to the control groups, the relative activities of the cells expressing high and low ZBTB7A were suppressed by 2-DG. In particular, the relative activities of RNAi-5-8F with 2-DG were suppressed (Figs. 4A–4H).

ZBTB7A directly suppresses GLUT1 expression

Using bioinformatic tools, the GLUT1 sequence from −857 to −845 (GCCAGGAACTCGC) was predicted (Fig. 5A). Dual-luciferase reporter assays and ChIP–qPCR were used to confirm the interaction between ZBTB7A and GLUT1 *in vitro*. The former assay suggested that ZBTB7A suppressed the expression of GLUT1 (Fig. 5B). The latter revealed the direct binding of ZBTB7A to the GLUT1 promoter (Fig. 5C).

ZBTB7A knockdown enhances 2-deoxy-d-glucose-mediated suppression of glycolysis in vivo

Compared to the control groups, the xenograft model of RNAi-5-8F suppressed by 2-DG exhibited reduced a level of glycolysis; in the group, the volumes and weights of the tumors were smaller and lighter, respectively, than those of the other groups (Figs. 6A and 6B). The expression of GLUT1 protein was suppressed in the RNAi-5-8F cells treated with 2-DG (Fig. 6C). The results indicated an enhanced dependency of ZBTB7A-knockdown tumors, which were more vulnerable to 2-DG than ZBTB7A overexpressing tumors (Fig. 6D).

Discussion

ZBTB7A, or Pokemon, showed complex characteristics and was expressed at different levels in NPC cells. 5-8F and

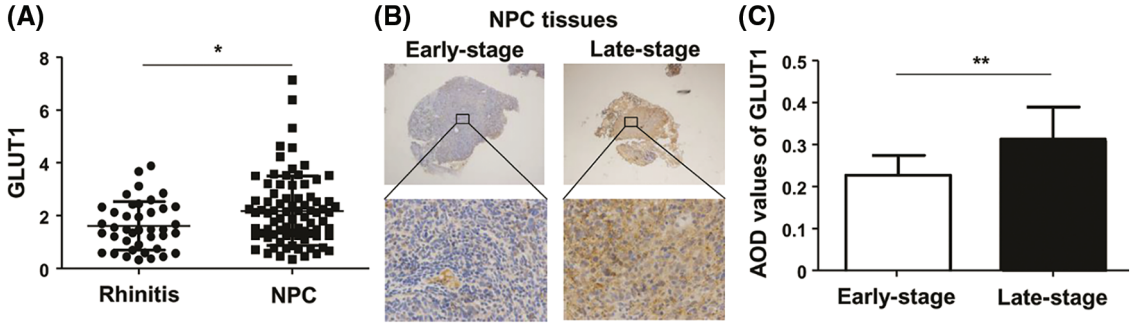

FIGURE 1. The expression of GLUT1 in NPC tissues. (A) GLUT1 expression in 80 NPC tissues and 40 controls was detected by quantitative real-time polymerase chain reaction. (B) GLUT1 expression in 14 late-stage and 10 early-stage NPC tissues was detected by immunohistochemistry (upper: 40×; lower: 400×). (C) The bar charts represent AOD values of GLUT1 in the early and late stages of NPC. * $P < 0.05$ and ** $P < 0.01$.

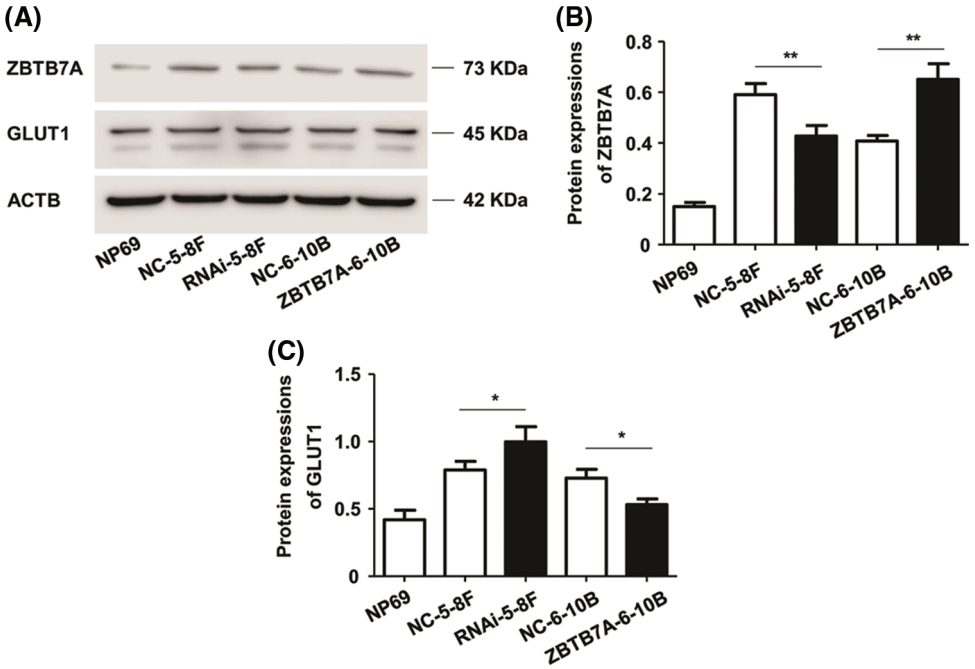

FIGURE 2. The expression of ZBTB7A and GLUT1 in NPC cells stably transfected with lentiviruses. (A) The bands represent the expression of ZBTB7A, GLUT1, and ACTB proteins in the cells. (B) and (C) The bar charts represent the expression levels of ZBTB7A and GLUT1 in the cells, respectively. * $P < 0.05$ and ** $P < 0.01$.

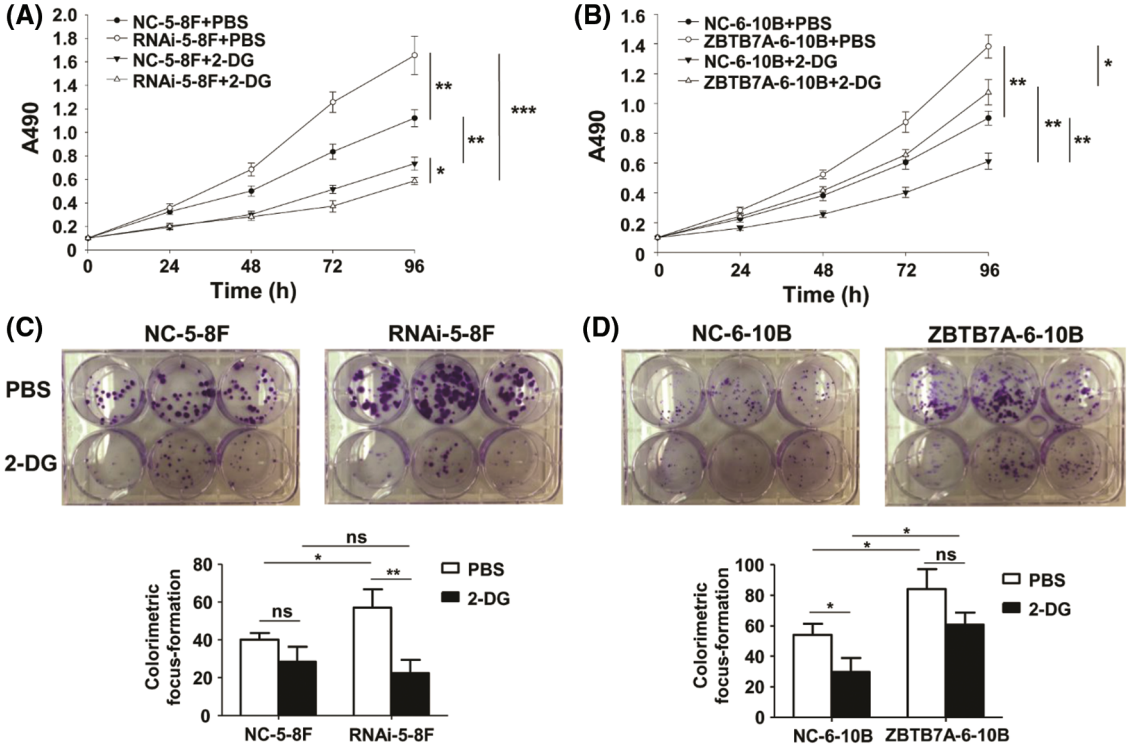

FIGURE 3. The vitality and proliferation of NPC cells stably transfected with lentiviruses were tested by 2-DG. (A) and (B) The vitality of the cells was detected by MTT assay. The different groups were compared at 96 h. (C) and (D) The proliferation of the cells was detected by colorimetric focus forming assay. * $P < 0.05$, ** $P < 0.01$ and *** $P < 0.001$; ns: nonsense.

6-10B cells were used as the research objects because of their high and low metastatic potential, respectively (Li *et al.*, 2021). WB assays showed that ZBTB7A expression in 5-8F was higher than in 6-10B cells (Liu *et al.*, 2019). Cells were stably transfected with lentiviruses, and ZBTB7A was effectively knocked down in 5-8F cells and overexpressed in 6-10B cells. The induction or reduction of GLUT1 secondary to the ZBTB7A intervention was also limited.

Compared to earlier published results (Liu *et al.*, 2019; Liu *et al.*, 2018), the vitalities of RNAi-5-8F and ZBTB7A-6-10B were still stronger than those of NC-5-8F and NC-6-10B, respectively. These contradictory characteristics

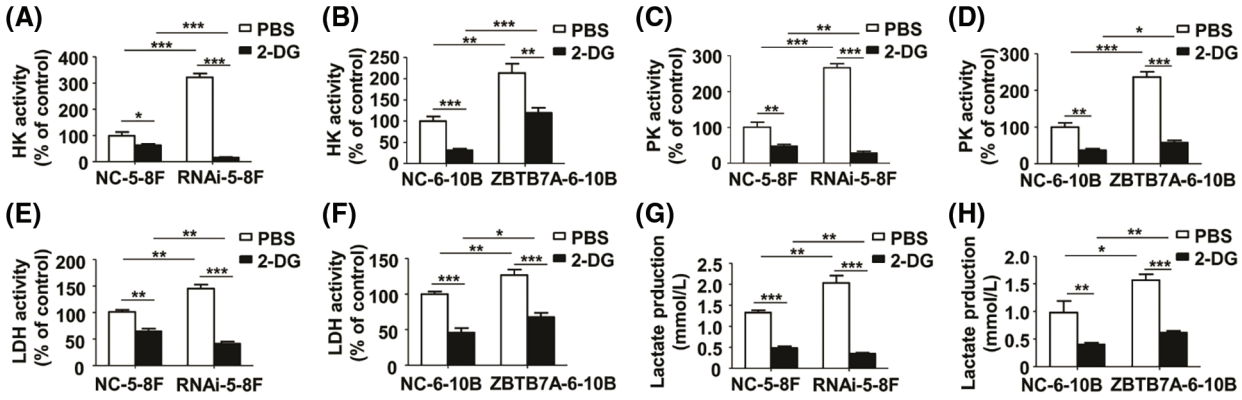

FIGURE 4. The activities of key glycolysis enzymes and lactate production in NPC cells stably transfected with lentiviruses were measured by 2-deoxy-d-glucose (2-DG). (A) and (B) The HK activity of the cells. (C) and (D) The PK activity of the cells. (E) and (F) The LDH activity of the cells. (G) and (H) The lactate production in the cells. * $P < 0.05$, ** $P < 0.01$ and *** $P < 0.001$.

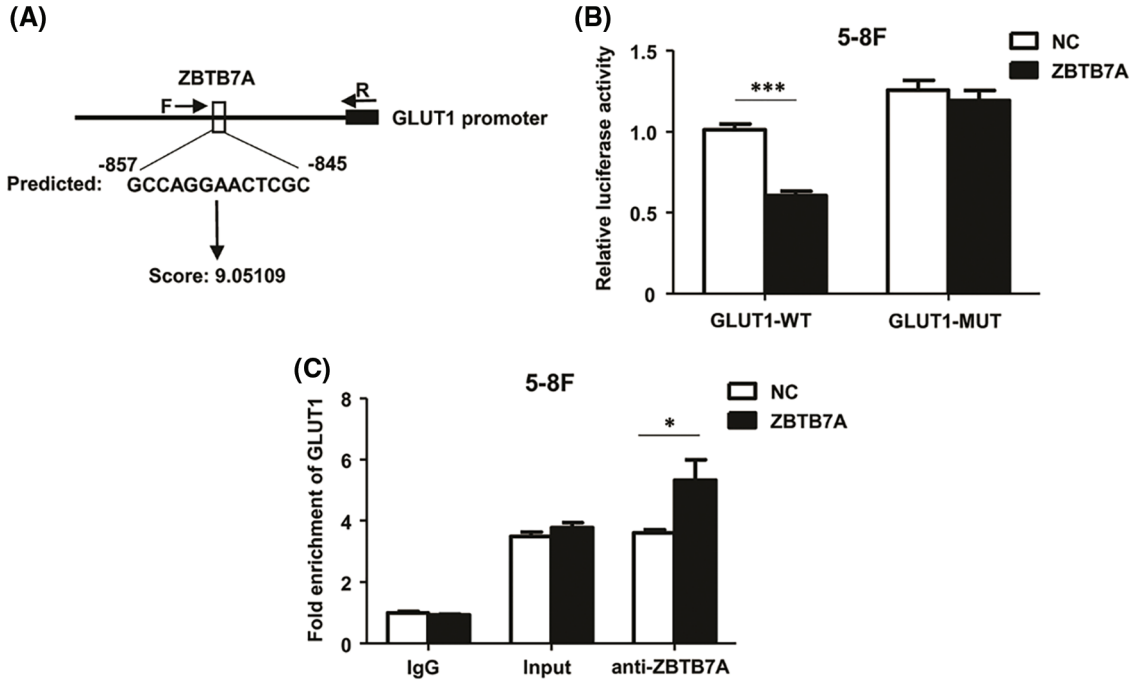

FIGURE 5. ZBTB7A directly suppressed GLUT1 expression by binding to the promoter region of GLUT1. (A) A potential interaction between ZBTB7A and the promoter region of GLUT1 was predicted by JASPAR software. To generate luciferase reporter constructs, the forward primers (F: 5'-TGTAAGGCAAGCTGGGATG-3') and reverese primer (R: 5'-GGTCTTTCTACAACCCTACGAG-3') were used to amplify part of the GLUT1 promoter region. (B) A dual-luciferase reporter assay was used to analyze the potential interaction between ZBTB7A and GLUT1. (C) Chromatin immunoprecipitation-quantitative real-time polymerase chain reaction was used to analyze whether ZBTB7A is directly bound to the GLUT1 promoter. * $P < 0.05$ and *** $P < 0.001$.

indicate that different expression levels of ZBTB7A influence complex regulatory networks to maintain the growth of NPC cells. The idea of blocking NPC cells was probably unsuccessful because ZBTB7A could only be knocked down. Some genes do not simply promote or suppress cancer progression. Although overexpression of solute carrier family 27 member 6 inhibits NPC growth *in vitro* and *in vivo*, it enhances the metastatic ability of NPC cells (Zhong *et al.*, 2022). Cyclin-dependent kinase 12 promotes tumorigenesis but induces vulnerability for breast cancer therapy via inhibiting folate one-carbon metabolism (Filippone *et al.*, 2022).

In this study, the knockdown and overexpression of ZBTB7A in different cells led to identical phenotypes and metabolic profiles. Surprisingly, the vitality and proliferation of the cells expressing low levels of ZBTB7A were dramatically suppressed by 2-DG. The cells expressing high levels of ZBTB7A were not very sensitive to 2-DG. Moreover, the growth of RNAi-5-8F xenografts was effectively suppressed by 2-DG. This result was similar to that in human colon carcinoma shZBTB7A-HCT116 cells treated with 2-DG *in vivo* (Liu *et al.*, 2014).

HK, PK, and LDH are the key enzymes of glycolysis. 2-DG acts as a D-glucose mimic and inhibits glycolysis due to the formation and intracellular accumulation of 2-deoxy-d-glucose-6-phosphate, and hampers the function of HK and glucose-6-phosphate isomerase (Pajak *et al.*, 2019; Raman *et al.*, 2022). The definite mechanisms by which 2-DG inhibits

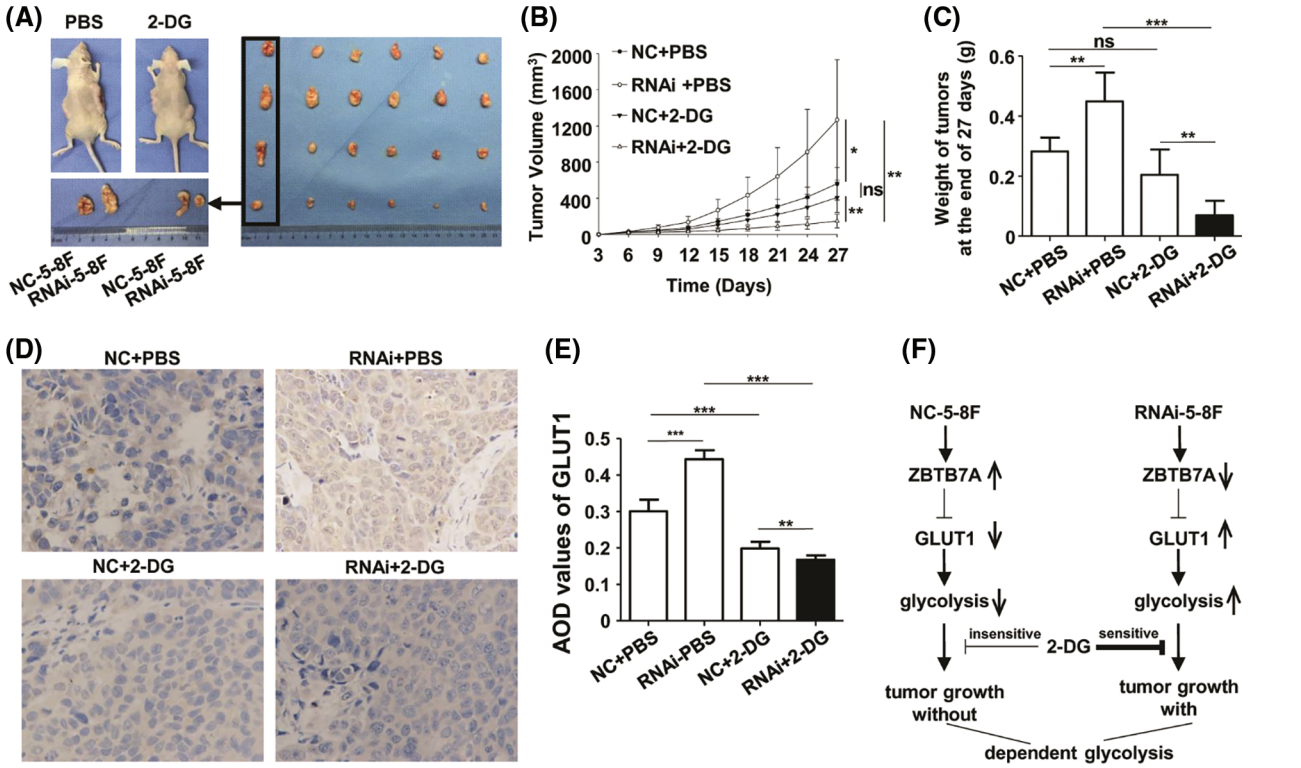

FIGURE 6. The cells with stable ZBTB7A knockdown were tested by 2-deoxy-d-glucose (2-DG) in xenografts. (A) The primary tumors due to RNAi-5-8F and NC-5-8F in phosphate-buffered saline (PBS) and 2-DG are shown on a desk. NC-5-8F and RNAi-5-8F cells were injected into the left and right flanks, respectively, of 24 mice. Then they were randomly grouped and injected with PBS and 2-DG (left). Tumor masses were arranged into four groups (raw/group), named NC-5-8F+PBS, RNAi-5-8F+PBS, NC-5-8F+2-DG, and RNAi-5-8F+2-DG (right). (B) The volumes and weights of the tumors were measured and compared on day 27. (C) GLUT1 expression in the tumor masses was detected by IHC (400×). (D) The regulatory mechanism of the cells with stable knockdown of ZBTB7A with glycolysis is shown. * $P < 0.05$, ** $P < 0.01$ and *** $P < 0.001$; ns: nonsense.

PK and LDH have not been determined. While 2-DG had no obvious effects on the total level of PK muscle isoenzyme M2 (PKM2) in a mouse model of inflammatory lung injury (Hu *et al.*, 2018), it inhibited the release of LDH in the rat tubular cell line NRK-52E (Ouyang *et al.*, 2015). The activities of HK, PK, and LDH were suppressed by 2-DG in cells expressing low levels of ZBTB7A. Among all cells used in this study, RNAi-5-8F cells had lactate production that was reduced to its lowest level by 2-DG the most.

Furthermore, the potential connection between ZBTB7A and GLUT1 provides a possible pathway for inhibiting NPC (Liu *et al.*, 2019). Reprogramming cellular metabolism has been demonstrated to facilitate tumorigenesis (Hanahan, 2022). GLUT1, a key enzyme of metabolic reprogramming, is closely associated with glycolysis (Wang *et al.*, 2022). In this study, we confirmed via a dual-luciferase reporter assay and ChIP–qPCR that high expression of GLUT1 was associated with late-stage NPC and that ZBTB7A directly suppressed GLUT1 expression. The regulatory mechanism warrants studying and developing trial therapies.

Conclusion

In tumors of highly metastatic cells, we consider that targeted therapy of key genes related to NPC progression is not simple. NPC cells can be weakened through overexpression or knockdown of targeted genes. This study revealed that ZBTB7A controls the 2-DG-induced inhibition of glycolysis by affecting GLUT1 expression. This conclusion suggests that the combination of targeted therapy and metabolic chemotherapy could halt NPC progression.

Acknowledgement: We are very grateful to Professor Sai-Wah Tsao from the University of Hong Kong for generously sharing with us the cell line NP69 and to Professor Musheng Zeng from Sun Yat-sen University for kindly providing 5-8F and 6-10B cells.

Availability of Data and Materials: All data generated or analyzed during this study are included in this published article and its supplementary information files.

Author Contributions: Conception and design: Wei Jiao, Fei Liu, and Shenhong Qu; administrative support: Shenhong Qu and Wei Jiao; provision of study materials or patients: Yongli Wang, Fengzhu Tang, Bing Li, Min Li, Jingjin Weng; performing experiments: Fei Liu, Yongli Wang, Jiaxiang Ye, Cheng Su, Mingzheng Mo, Weiming Deng, Wenlin Huang, and Linsong Ye; data analysis and interpretation: Fei Liu, Jiazhang Wei, and Jiao Lan; manuscript writing: Fei Liu and Jiazhang Wei. Final approval of manuscript: All authors.

Ethics Approval: The clinical samples were approved by the Ethics Committee of The People's Hospital of Guangxi Zhuang Autonomous Region, Guangxi Academy of Medical Sciences (Ethical Application Ref: Keyan-Guangxi-Keji-2016-20; Date of Approval: May 4th, 2016). The BALB/c mice were

approved by the Ethics Committee of Guangxi Medical University Laboratory Animal Centre (Ethical Application Ref: 202007059; Date of Approval: July 16th, 2020).

Funding Statement: The study was supported by the Natural Science Foundation of Guangxi Province (2016GXNSFBA380144), Guangxi Science and Technology Base and Talent Project (GuiKe-AD20297069) and National Natural Science Foundation of China (81960493).

Conflicts of Interest: The authors declare that they have no conflicts of interest to report regarding the present study.

References

Badoual C (2022). Update from the 5th edition of the world health organization classification of head and neck tumors: Oropharynx and nasopharynx. *Head and Neck Pathology* **16**: 19–30. DOI 10.1007/s12105-022-01449-2.

Chen Y, Chang ET, Liu Z, Liu Q, Cai Y et al. (2021a). Residence characteristics and risk of nasopharyngeal carcinoma in Southern China: Of population based case control study. *Environment International* **151**: 106455. DOI 10.1016/j.envint.2021.106455.

Chen YP, Ismaila N, Chua MLK, Colevas AD, Haddad RB et al. (2021b). Chemotherapy in combination with radiotherapy for definitive-intent treatment of stage II–IVA nasopharyngeal carcinoma: CSCO and ASCO Guideline. *Journal of Clinical Oncology* **39**: 840–859. DOI 10.1200/JCO.20.03237.

DeCaprio J, Kohl TO (2020). Chromatin immunoprecipitation. *Cold Spring Harbor Protocols* **2020**: 98665. DOI 10.1101/pdb.prot098665.

Filippone MG, Gaglio D, Bonfanti R, Tucci FA, Ceccacci E et al. (2022). CDK12 promotes tumorigenesis but induces vulnerability to therapies inhibiting folate one-carbon metabolism in breast cancer. *Nature Communications* **13**: 2642. DOI 10.1038/s41467-022-30375-8.

Geng R, Zheng Y, Zhou D, Li Q, Li R et al. (2020). ZBTB7A, a potential biomarker for prognosis and immune infiltrates, inhibits progression of endometrial cancer based on bioinformatics analysis and experiments. *Cancer Cell International* **20**: 542. DOI 10.1186/s12935-020-01600-5.

Hanahan D (2022). Hallmarks of cancer: New dimensions. *Cancer Discovery* **12**: 31–46. DOI 10.1158/2159-8290.CD-21-1059.

Hong X, Liu N, Liang Y, He Q, Yang X et al. (2020). Circular RNA CRIM1 functions as a ceRNA to promote nasopharyngeal carcinoma metastasis and docetaxel chemoresistance through upregulating FOXQ1. *Molecular Cancer* **19**: 33. DOI 10.1186/s12943-020-01149-x.

Hu K, Yang Y, Lin L, Ai Q, Dai J et al. (2018). Caloric restriction mimetic 2-deoxyglucose alleviated inflammatory lung injury via suppressing nuclear pyruvate kinase M2-signal transducer and activator of transcription 3 pathway. *Frontiers in Immunology* **9**: 426. DOI 10.3389/fimmu.2018.00426.

Jiao W, Liu F, Tang FZ, Lan J, Xiao RP et al. (2013). Expression of the Pokemon proto-oncogene in nasopharyngeal carcinoma cell lines and tissues. *Asian Pacific Journal of Cancer Prevention* **14**: 6315–6319. DOI 10.7314/APJCP.2013.14.11.6315.

Kong J, Liu X, Li X, Wu J, Wu N et al. (2016). Pokemon promotes the invasiveness of hepatocellular carcinoma by enhancing MEF2D transcription. *Hepatology International* **10**: 493–500. DOI 10.1007/s12072-015-9697-y.

Li M, Peng F, Wang G, Liang X, Shao M et al. (2021). Coupling of cell surface biotinylation and SILAC-based quantitative proteomics identified myoferlin as a potential therapeutic target for nasopharyngeal carcinoma metastasis. *Frontiers in Cell and Developmental Biology* **9**: 621810. DOI 10.3389/fcell.2021.621810.

Liu F, Lan J, Jiao W, Mo X, Huang Y et al. (2017). Differences in Zbtb7a expression cause heterogeneous changes in human nasopharyngeal carcinoma CNE3 sublines. *Oncology Letters* **14**: 2669–2676. DOI 10.3892/ol.2017.6553.

Liu F, Tang F, Lan J, Jiao W, Si Y et al. (2018). Stable knockdown of ZBTB7A promotes cell proliferation and progression in nasopharyngeal carcinoma. *Tumori Journal* **104**: 37–42. DOI 10.5301/tj.5000706.

Liu F, Wei J, Hao Y, Lan J, Li W et al. (2021a). Long intergenic non-protein coding RNA 02570 promotes nasopharyngeal carcinoma progression by adsorbing microRNA miR-4649-3p thereby upregulating both sterol regulatory element binding protein 1, and fatty acid synthase. *Bioengineered* **12**: 7119–7130. DOI 10.1080/21655979.2021.1979317.

Liu F, Wei J, Hao Y, Tang F, Jiao W et al. (2019). Long noncoding RNAs and messenger RNAs expression profiles potentially regulated by ZBTB7A in nasopharyngeal carcinoma. *Biomed Research International* **2019**: 7246491. DOI 10.1155/2019/7246491.

Liu L, Liu S, Deng P, Liang Y, Xiao R et al. (2021b). Targeting the IRAK1-S100A9 axis overcomes resistance to paclitaxel in nasopharyngeal carcinoma. *Cancer Research* **81**: 1413–1425. DOI 10.1158/0008-5472.CAN-20-2125.

Liu XS, Genet MD, Haines JE, Mehanna EK, Wu S et al. (2015). ZBTB7A suppresses melanoma metastasis by transcriptionally repressing MCAM. *Molecular Cancer Research* **13**: 1206–1217. DOI 10.1158/1541-7786.MCR-15-0169.

Liu XS, Haines JE, Mehanna EK, Genet MD, Ben-Sahra I et al. (2014). ZBTB7A acts as a tumor suppressor through the transcriptional repression of glycolysis. *Genes Development* **28**: 1917–1928. DOI 10.1101/gad.245910.114.

Liu YP, Wen YH, Tang J, Wei Y, You R et al. (2021c). Endoscopic surgery compared with intensity-modulated radiotherapy in resectable locally recurrent nasopharyngeal carcinoma: A multicentre, open-label, randomised, controlled, phase 3 trial. *The Lancet Oncology* **22**: 381–390. DOI 10.1016/S1470-2045(20)30673-2.

Mao A, Chen M, Qin Q, Liang Z, Jiang W et al. (2019). ZBTB7A promotes migration, invasion and metastasis of human breast cancer cells through NF-κB-induced epithelial-mesenchymal transition *in vitro* and *in vivo*. *The Journal of Biochemistry* **166**: 485–493. DOI 10.1093/jb/mvz062.

Ouyang Z, Cao W, Zhu S, Liu X, Zhong Z et al. (2015). Protective effect of 2-deoxy-D-glucose on the cytotoxicity of cyclosporin A *in vitro*. *Molecular Medicine Reports* **12**: 2814–2820. DOI 10.3892/mmr.2015.3777.

Pajak B, Siwiak E, Sołtyka M, Priebe A, Zieliński R et al. (2019). 2-deoxy-d-glucose and its analogs: from diagnostic to therapeutic agents. *International Journal of Molecular Sciences* **21**: 234. DOI 10.3390/ijms21010234.

Peng H, Zhang J, Zhang PP, Chen L, Tang LL et al. (2019). ARNTL hypermethylation promotes tumorigenesis and inhibits cisplatin sensitivity by activating CDK5 transcription in nasopharyngeal carcinoma. *Journal of Experimental & Clinical Cancer Research* **38**: 11. DOI 10.1186/s13046-018-0997-7.

Raman APS, Kumari K, Jain P, Vishvakarma VK, Kumar A et al. (2022). *In silico* evaluation of binding of 2-deoxy-d-glucose with mpro of nCoV to combat COVID-19. *Pharmaceutics* **14**: 135. DOI 10.3390/pharmaceutics14010135.

Sena-Esteves M, Gao G (2018). Production of high-titer retrovirus and lentivirus vectors. *Cold Spring Harbor Protocols* **2018**: 273–280. DOI 10.1101/pdb.prot095687.

Stepanenko AA, Heng HH (2017). Transient and stable vector transfection: Pitfalls, off-target effects, artifacts. *Mutation Research/Reviews in Mutation Research* **773**: 91–103. DOI 10.1016/j.mrrev.2017.05.002.

Sun G, Peng B, Xie Q, Ruan J, Liang X (2018). Upregulation of ZBTB7A exhibits a tumor suppressive role in gastric cancer cells. *Molecular Medicine Reports* **17**: 2635–2641. DOI 10.3892/mmr.2017.8104.

Wang G, Lunardi A, Zhang J, Chen Z, Ala U et al. (2013). Zbta7a suppresses prostate cancer through repression of a Sox9-dependent pathway for cellular senescence bypass and tumor invasion. *Nature Genetics* **45**: 739–746. DOI 10.1038/ng.2654.

Wang L, Lin Y, Zhou X, Chen Y, Li X et al. (2022). CYLD deficiency enhances metabolic reprogramming and tumor progression in nasopharyngeal carcinoma via PFKFB3. *Cancer Letters* **532**: 215586. DOI 10.1016/j.canlet.2022.215586.

Wang L, Zhang MX, Zhang MF, Tu ZW (2020). ZBTB7A functioned as an oncogene in colorectal cancer. *BMC Gastroenterology* **20**: 370. DOI 10.1186/s12876-020-01456-z.

Xu M, Yao Y, Chen H, Zhang S, Cao SM et al. (2019). Genome sequencing analysis identifies Epstein-Barr virus subtypes associated with high risk of nasopharyngeal carcinoma. *Nature Genetics* **51**: 1131–1136. DOI 10.1038/s41588-019-0436-5.

Yeh LY, Yang CC, Wu HL, Kao SY, Liu CJ et al. (2020). The miR-372-ZBTB7A oncogenic axis suppresses TRAIL-R2 associated drug sensitivity in oral carcinoma. *Frontiers in Oncology* **10**: 47. DOI 10.3389/fonc.2020.00047.

Zhang B, Cui B, Du J, Shen X, Wang K et al. (2019). ATR activated by EB virus facilitates chemotherapy resistance to cisplatin or 5-fluorouracil in human nasopharyngeal carcinoma. *Cancer Management and Research* **11**: 573–585. DOI 10.2147/CMAR.S187099.

Zhang L, Wang Y, Zhang L, Xia X, Chao Y et al. (2019). ZBTB7A, a miR-663a target gene, protects osteosarcoma from endoplasmic reticulum stress-induced apoptosis by suppressing LncRNA GAS5 expression. *Cancer Letters* **448**: 105–116. DOI 10.1016/j.canlet.2019.01.046.

Zhang Z, Guan B, Li Y, He Q, Li X et al. (2021). Increased phosphorylated CREB1 protein correlates with poor prognosis in clear cell renal cell carcinoma. *Translational Andrology and Urology* **10**: 3348–3357. DOI 10.21037/tau-21-371.

Zhao Z, Wang J, Wang S, Chang H, Zhang T et al. (2017). LncRNA CCAT2 promotes tumorigenesis by over-expressed Pokemon in non-small cell lung cancer. *Biomedicine & Pharmacotherapy* **87**: 692–697. DOI 10.1016/j.biopha.2016.12.122.

Zhong X, Yang Y, Li B, Liang P, Huang Y et al. (2022). Downregulation of SLC27A6 by DNA hypermethylation promotes proliferation but suppresses metastasis of nasopharyngeal carcinoma through modulating lipid metabolism. *Frontiers in Oncology* **11**: 780410. DOI 10.3389/fonc.2021.780410.

Zhu X, Cong J, Lin Z, Sun J, Yang B et al. (2020). Inhibition of HMGB1 overcomes resistance to radiation and chemotherapy in nasopharyngeal carcinoma. *OncoTargets and Therapy* **13**: 4189–4199. DOI 10.2147/OTT.S239243.

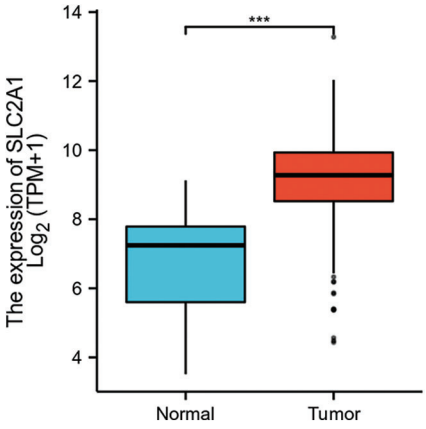

SUPPLEMENTARY FIGURE S1. The RNA expression of SLC2A1 (GLUT1) in HNSCC.

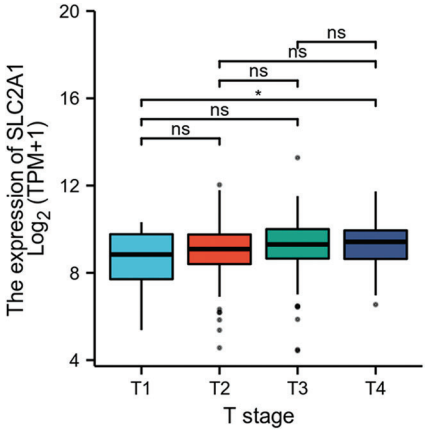

SUPPLEMENTARY FIGURE S2. SLC2A1 expression in HNSCC patients in early or late clinical stages.

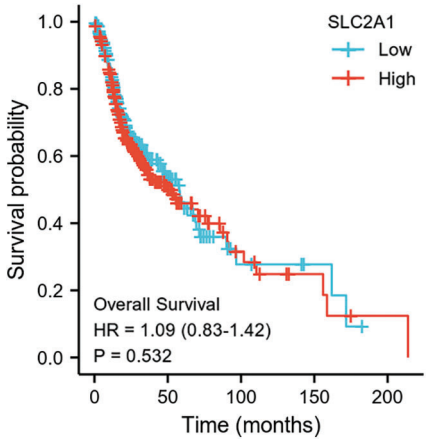

SUPPLEMENTARY FIGURE S3. Overall survival among HNSCC patients with high or low SLC2A1 expression.

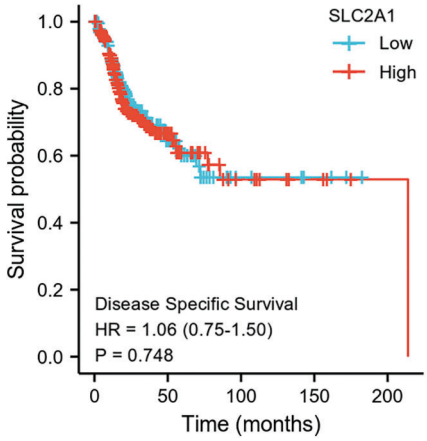

SUPPLEMENTARY FIGURE S4. Disease-specific survival among HNSCC patients with high or low SLC2A1 expression.

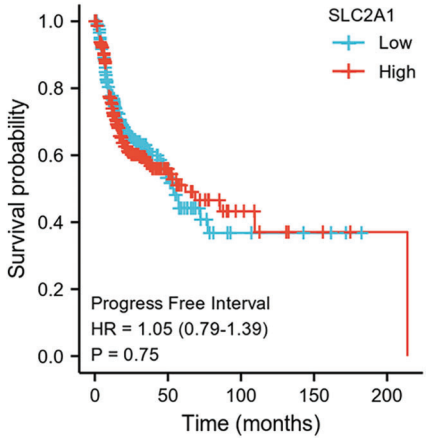

SUPPLEMENTARY FIGURE S5. Progression-free interval among HNSCC patients with high or low SLC2A1 expression.

SUPPLEMENTARY FIGURE S6. The correlation between ZBTB7A and SLC2A1 expression in HNSCC.

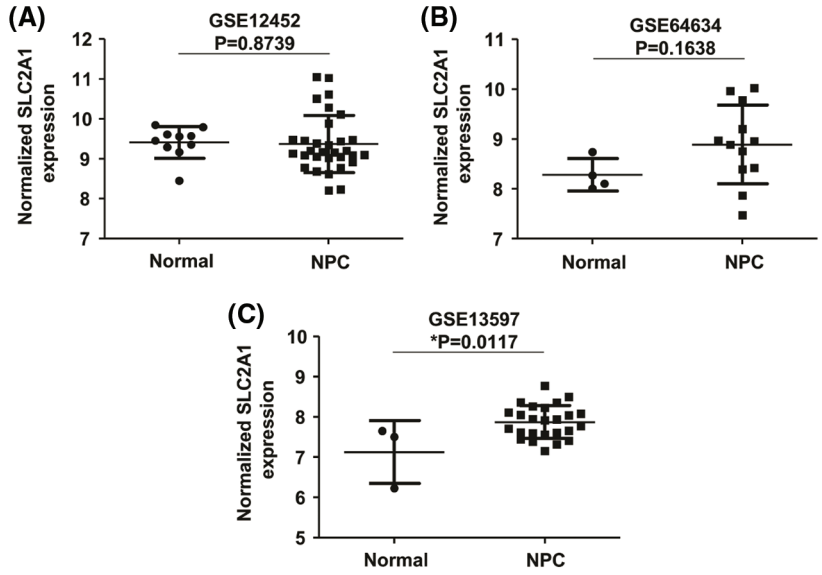

SUPPLEMENTARY FIGURE S7. The relative expression of SLC2A1 in NPC.